Magnetic Resonance in Medicine 41:1246–1254 (1999)

QUIPSS II With Thin-Slice TI_1 Periodic Saturation: A Method for Improving Accuracy of Quantitative Perfusion Imaging Using Pulsed Arterial Spin Labeling

Wen-Ming Luh,[1] Eric C. Wong,[2] Peter A. Bandettini,[1] and James S. Hyde[1]*

Quantitative imaging of perfusion using a single subtraction, second version (QUIPSS II) is a pulsed arterial spin labeling (ASL) technique for improving the quantitation of perfusion imaging by minimizing two major systematic errors: the variable transit delay from the distal edge of the tagged region to the imaging slices, and the contamination by intravascular signal from tagged blood that flows through the imaging slices. However, residual errors remain due to incomplete saturation of spins over the slab-shaped tagged region by the QUIPSS II saturation pulse, and spatial mismatch of the distal edge of the saturation and inversion slice profiles. By replacing the original QUIPSS II saturation pulse with a train of thin-slice periodic saturation pulses applied at the distal end of the tagged region, the accuracy of perfusion quantitation is improved. Results of single and multislice studies are reported. Magn Reson Med 41:1246–1254, 1999. © **1999 Wiley-Liss, Inc.**

Key words: perfusion; arterial spin labeling; pulsed ASL; QUIPSS II

MRI-based arterial spin labeling (ASL) techniques use water in arterial blood as a freely diffusible tracer to measure perfusion noninvasively. Potentially, quantitative perfusion maps can be obtained that will be clinically useful. These methods can also be used to map brain function and to clarify functional MRI mechanisms. It is possible that ASL contrast will provide better localization of the sites of neuronal activity than blood oxygenation level-dependent (BOLD) contrast (1–3).

ASL techniques can be classified as continuous (4–9) and pulsed (10–20). In the former, the magnetization of arterial blood is continuously inverted by constant radiofrequency (RF) radiation in the presence of a constant gradient as it flows across the tagging plane (21). In the latter, the magnetization of a slab of arterial blood spins is inverted by an adiabatic hyperbolic secant (sech) pulse (22). In both approaches, the tag state is alternated with a control state in which the magnetization of arterial blood is not inverted, and the difference signal (control–tag) is proportional to perfusion. At higher field strengths, the ASL signal-to-noise ratio (SNR) increases not only because of higher sensitivity but also because of the longer T_1 of blood and tissue. However, continuous ASL techniques may be compromised at field strengths higher than 1.5 T in human brain studies by RF power deposition limits.

Quantitative imaging of perfusion using a single subtraction, second version (QUIPSS II), which is based on the conventional pulsed ASL techniques such as echoplanar imaging and signal targeting with alternating RF (EPISTAR; 10–12), flow-sensitive alternating inversion recovery (FAIR; 13–16), and proximal inversion with a control for off-resonance effects (PICORE; 18,19), was introduced by Wong et al (17–20) to minimize the systematic errors in the quantitation of perfusion caused by the spatially varying transit delay (δt) and the ''flow-through'' effect (19,20). In this method a 15-lobe sinc saturation pulse is applied in the tagged region at time TI_1 after the inversion pulse and before image acquisition. An additional advantage of QUIPSS II is that it can be applied in multislice mode. In the previous implementation of QUIPSS II (17–19), two sources of residual errors occur. The first is incomplete saturation of spins over the slab-shaped tagged region by the QUIPSS II saturation pulse. Unlike the sech slice profile, the slice profile of a sinc-shaped pulse is subject to B_1 inhomogeneity. For a thick axial slice as used in QUIPSS II, through-plane B_1 homogeneity is generally worse than in-plane B_1 homogeneity using a typical head RF coil. Incomplete saturation of the spins of tagged blood leads to overestimation of perfusion. The second source of error arises from spatial mismatch of the distal edge of the saturation and inversion slice profiles. The sech inversion tagging pulse used in pulsed ASL methods results in a highly selective inversion of magnetization with sharp edges that the slice profile of the QUIPSS II saturation pulse does not match.

Here we describe a method to minimize these errors. The idea is to replace the QUIPSS II saturation pulse by a periodic train of thin-slice saturation pulses at the distal end of the tagged region. This method addresses both of the sources of error of QUIPSS II. The purpose of the QUIPSS II saturation pulse is to saturate spins that remain in the tagged region at time TI_1. Since all tagged spins must flow through the thin-slice region using the method described in this paper, they can be saturated by the train of thin-slice pulses. A thin sinc slice profile has sharper edges than a thick one and therefore has a better match to the distal edge of the inversion profile. In addition, a thin-slice pulse has greater B_1 homogeneity over the slice thickness than a thick-slice pulse. By applying QUIPSS II with thin-slice TI_1 periodic saturation (Q2TIPS), the accuracy of perfusion measurements is improved. Preliminary data using this technique were previously reported in abstract form (23).

[1]Biophysics Research Institute, Medical College of Wisconsin, Milwaukee, Wisconsin.

[2]Departments of Radiology and Psychiatry, University of California, San Diego, San Diego, California.

Grant sponsor: National Institutes of Health; Grant numbers: MH51358 and NS36211.

*Correspondence to: James S. Hyde, Biophysics Research Institute, Medical College of Wisconsin, Milwaukee, WI 53226. E-mail: jshyde@mcw.edu

Received 31 July 1998; revised 21 January 1999; accepted 24 February 1999.

MATERIALS AND METHODS

Q2TIPS

Images were acquired using a 3T Bruker Biospec 30/60 scanner (Bruker Medical, Karlsruhe, Germany) on normal volunteers. A three-axis local head gradient coil fitted with an endcapped quadrature birdcage RF coil was used. Figure 1 shows the Q2TIPS pulse sequence and positions of the in-plane presaturation slab, the inversion-tagged region, the periodic saturation slice, and the imaging slices. The PICORE tagging scheme was used, although EPISTAR and FAIR can also be used, with a 10-cm tagged region created by a 15-msec adiabatic sech pulse (22) with parameters $\mu = 10$ and $\beta = 800\ s^{-1}$ positioned with a 1-cm gap relative to the proximal edge of the imaging slices (24). Two in-plane presaturation pulses were applied in the imaging slices as in PICORE and EPISTAR immediately before the inversion pulse to improve the cancellation of signal from static tissues between tag and control states. Single-shot blipped EPI acquisition was used with 24-cm FOV, 64×64 matrix, and 8-mm slice thickness.

The original QUIPSS II saturation pulse was replaced by a number of thin-slice sinc pulses applied periodically from TI_1 to TI_{1S} (TI_1 stop time) at the distal end of the tagged region. The purpose is to obtain improved saturation on the remaining part of the tag (tagged blood still in the tagged region at time TI_1) and a better matched slice profile at the distal edge of the tagged region. To be insensitive to δt, only the distal edge of the inversion and saturation slice profiles must be matched since δt is the time for the tagged blood to reach the imaging voxels from the distal edge of the tagged region. The tagged blood will be saturated if the normal component of velocity of the tagged blood passing through the periodic saturation slice is less than the "cut-off" velocity (V_c), which is defined by

$$V_c = \frac{S_{nom}}{T_p} = \frac{S_{nom}(N_p - 1)}{TI_{1S} - TI_1} \quad [1]$$

where S_{nom} is the nominal slice thickness of the periodic saturation pulses, T_p is the interval between successive periodic saturation pulses, and N_p is the number of periodic saturation pulses.

In the previous implementation of QUIPSS II (17–19), a 15-lobe sinc pulse was used for TI_1 saturation. However, because the tagged region is usually thick (i.e., 10 cm), the incomplete effectiveness of the QUIPSS II saturation pulse renders part of the saturated tag visible as perfusion signal and causes overestimation of regional cerebral blood flow (CBF), as evidenced from the positive intercept of the QUIPSS II signal vs. TI_1 curve (17).

The longitudinal magnetization of the tagged blood spins as a function of time in a QUIPSS II (or Q2TIPS) experiment is illustrated in Fig. 2. The magnetization of tagged spins eventually perfusing the target tissue (solid line) is inverted at time zero and undergoes T_1 relaxation with $T_1 = T_{1B}$ (T_1 of blood). The T_1 relaxation time of the tagged spins shifts from T_{1B} to the T_1 of tissue (T_{1t}) when the tagged water spins exchange with brain parenchyma water spins in the capillary bed (open arrow). Note that the tagged spins may exchange with tissue spins at different times relative to the inversion pulse. During the control state the magnetization remains fully relaxed (dashed line). If the TI_1 saturation is effective, the magnetization of the tagged blood remaining in the tagged region at time TI_1 will be zero at time TI_1 (or between TI_1 and TI_{1S} for Q2TIPS) and will be the same for both tag and control states after TI_1. Thus, the signal from the saturated blood will be canceled

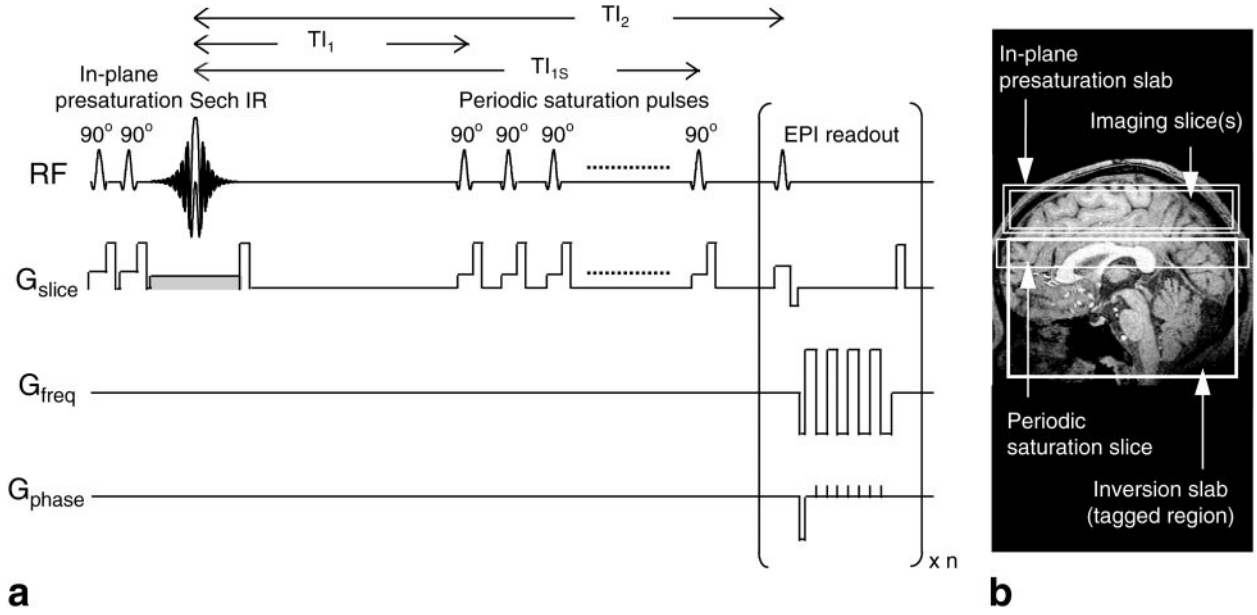

FIG. 1. **a:** Pulse sequence for Q2TIPS. Double in-plane presaturation pulses followed by the sech inversion tagging pulse. The gradient lobe in gray is alternately applied for tag and control states. Periodic saturation pulses applied from TI_1 to TI_{1S} consist of a train of 90° excitation pulses each followed by a crusher gradient. Single or multislice EPI acquisition is applied at TI_2. **b:** Locations of the in-plane presaturation slab, imaging slice(s), periodic saturation slice, and inversion slab used in the PICORE tagging scheme.

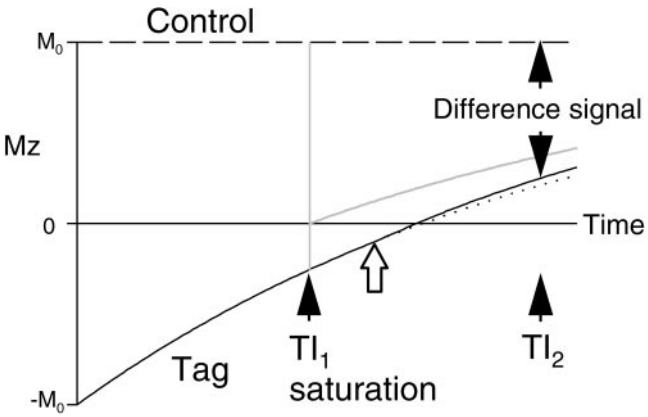

FIG. 2. Longitudinal magnetization of tagged blood as a function of time during the tag state (solid line) and control state (dashed line) in a QUIPSS II (or Q2TIPS) experiment. During the tag state, the magnetization is inverted at time zero and undergoes T_1 relaxation. The T_1 of the tagged spins shifts from T_{1B} to T_{1t} (open arrow) when the tagged water spins exchange with brain parenchyma water spins in the capillary bed. If the TI_1 saturation is effective, the difference signal between tag and control states at image acquisition time TI_2 will be proportional to perfusion. The magnetization of the tagged spins still in the tagged region at time TI_1 will be saturated to zero during both tag and control states and will then undergo saturation recovery (gray line). Thus the signal from the saturated spins will be cancelled in the subtraction.

in the subtraction. The difference signal ΔM (control − tag) will be proportional to CBF, as described previously in the kinetic model of Eqs. [2]–[5] (19,20,25,26):

$$\Delta M(TI_2) = 2\, M_{0B}\, f\, TI_1\, e^{-TI_2/T_{1B}}\, q(T_{1B}, T_{1t}, T_{ex}, f, \lambda, TI_2) \quad [2]$$

$$\text{for } TI_1 < \tau \quad \text{and} \quad TI_2 > TI_1 + \delta t \quad [3]$$

and

$$\Delta M(TI_2) = 2\, M_{0B}\, f\, \tau\, e^{-TI_2/T_{1B}}\, q(T_{1B}, T_{1t}, T_{ex}, f, \lambda, TI_2) \quad [4]$$

$$\text{for } TI_1 > \tau \quad \text{and} \quad TI_2 > \tau + \delta t \quad [5]$$

where M_{0B} is fully relaxed magnetization of arterial blood, f is the CBF in ml of blood/ml of issue/min, T_{ex} is the transit time from the distal edge of the tagged region to the capillary bed where tagged blood water exchanges with brain parenchyma water, λ is the tissue-to-blood partition coefficient of water, τ is the time width of the tag, and q is a correction factor that accounts for a shift in the T_1 decay of the tag due to exchange of tagged spins from blood into brain tissue, and clearance of the tag by venous outflow. Typically q is near unity and ΔM itself is a quantitative perfusion map. If M_{0B} and T_{1B} are known, the absolute perfusion can be calculated. It can be shown from Eqs. [2] and [4] that at fixed TI_2, ΔM is zero for $TI_1 = 0$, increases linearly as TI_1 increases, and becomes constant for $TI_1 > \tau$.

At a given value of V_c, a longer T_p value can be used, which results in a thicker S_{nom} (Eq. [1]) and lower RF power deposition. However, more sinc pulse sidelobes are needed to obtain a sharp-edge slice profile as S_{nom} increases. For long-duration sinc pulses, the improvement in slice profile is limited, and saturation of fast-flowing spins may not be effective. In addition, the slice profile of a sinc pulse is subject to B_1 inhomogeneity, an effect that increases with increase in S_{nom}. In the present studies, 3.2-msec three-lobe sinc pulses were used. Saturation is generally improved with multiple saturation pulses because the magnetization is proportional to $(\cos \alpha)^{Np}$ for N_p pulses where α is a local flip angle, resulting in a wide range of α values for which saturation is very effective. T_p was set to 25 msec. The estimated worst-case average SAR (specific absorption rate) was below the Food and Drug Administration (FDA) guideline. V_c was set to 80 cm/sec, and thus S_{nom} was 2 cm.

Q2TIPS vs. QUIPSS II

For comparison, a 12.8-msec 15-lobe sinc pulse with 10-cm slice thickness was used as the saturation pulse for QUIPSS II. The slice profiles of this pulse and of a 3.2-msec three-lobe sinc pulse of 2-cm slice thickness, both with Hamming window weighting, were simulated and measured. The slice profiles were generated by simulating the Bloch equations with direct numerical integration for a given RF pulse waveform and measured with a gradient-echo sequence with a TE of 10.2 msec, TR=1 sec, $\alpha = 90°$, and 256 × 256 matrix using a cylindrical phantom of length 22 cm.

Single-shot blipped spin-echo EPI acquisition was used with both Q2TIPS and QUIPSS II for single-slice studies with 55.3 msec TE and 2.5 sec TR. TI_2 was 1.4 sec, while TI_1 was varied from 0.25 to 1 sec, and TI_{1S} was set empirically to 1.225 sec to saturate the remaining part of the tag. N_p ranged from 10 to 40. Typically, 120 images (60 tag/control pairs) were acquired.

Multislice Q2TIPS

In multislice studies, five contiguous 8-mm axial slices were acquired, inferior to superior, sequentially every 68 msec using gradient-recalled EPI with 27.2 msec TE. The slices further away from the tagged region with longer transit delay were acquired at longer TI_2 so that Eq. [3] would be more likely to hold (19,20). In the present studies, TI_2 was 1.4 sec for the first slice and 1.67 sec for the last slice, while TI_1 was varied from 0.3 to 0.9 sec. Other imaging parameters were TI_{1S} = 1.2 sec, TR = 2.5 sec, and 100 repetitions.

Optimization of TI_{1S} and TR

To ensure complete saturation of the remaining part of the tag, periodic saturation pulses can be applied until just before image acquisition at TI_2. However, Eq. [2] assumes fully relaxed blood in the tagged region before each inversion pulse. The longer the TI_{1S}, the longer the minimum TR value that can be used and the lower the SNR per unit time. The optimal TI_{1S} value should be the time when the tail of the entire tag reaches the proximal edge of the periodic saturation slice. To determine the optimal TI_{1S}, TI_1 was held constant at 0.7 sec, TI_2 = 1.4 sec, and TR = 2.5 sec, while TI_{1S} was varied from 0.725 to 1.225 sec. For minimum TR studies, TI_1 was 0.7 sec, TI_{1S} = 1.05 sec, and TI_2 = 1.4 sec while TR was varied from 1.9 to 2.7 sec. For each data point, 100 images were acquired using single-shot

blipped spin-echo EPI with a single axial slice across motor cortex areas.

Data Processing

For each study, all raw images were first registered for bulk motion correction using the *imreg* program from the AFNI software package (27), and then averaged after pairwise subtraction to generate the ΔM perfusion maps. T_1 maps were obtained in each study using inversion recovery EPI (IR-EPI). The inversion time was varied logarithmically from 0.03 to 18.13 sec with 15 data points and a TR of 20 sec. Gray matter (GM) and white matter (WM) regions of interest (ROIs) were selected from the T_1 maps based on T_1. Signals from pixels within ROIs were averaged from the perfusion maps. Standard errors were calculated from the variance of the averaged signals in ROIs from the time series of the ΔM difference images.

Perfusion calculations were performed using Eq. [2] with an assumed T_{1B} of 1.5 sec. M_{0B} was estimated from the WM signal in a single-shot EPI image with infinite TR using the signal ratio of WM to blood in the sagittal sinus from a proton density-weighted image, and the weighting of T_2/T_2* relaxation at TE (20). Assumed values of T_2/T_2* of WM and blood were 80/40 and 200/100 msec, respectively. The correction factor q in Eq. [2] was assumed to be unity. If $T_{1B} = 1.5$ sec, $T_{1t} = 1.3$ sec, $T_{ex} = 0.9$ sec, $f = 60$ ml/100 ml/min, $\lambda = 0.9$, and $TI_2 = 1.4$ sec, then $q = 0.97$ (19). The calculated perfusion would be underestimated by 3%, which is less than the standard error of measurements (see results). For visual presentation, all 64×64 images were bilinearly interpolated to a 256×256 matrix.

RESULTS

Q2TIPS vs. QUIPSS II

Figure 3 shows the slice profiles obtained by simulation and by experimental measurements. In the simulated slice profiles, the three-lobe sinc pulse of 2-cm thickness has a sharper edge and better saturation at the distal end of the tagged region. The phantom slice profile of the three-lobe sinc pulse of 2-cm thickness closely resembles the simulated profile. However, the phantom slice profile of the 15-lobe sinc pulse of 10-cm thickness is much worse than the simulated one and varies from position to position due to B_1 inhomogeneity.

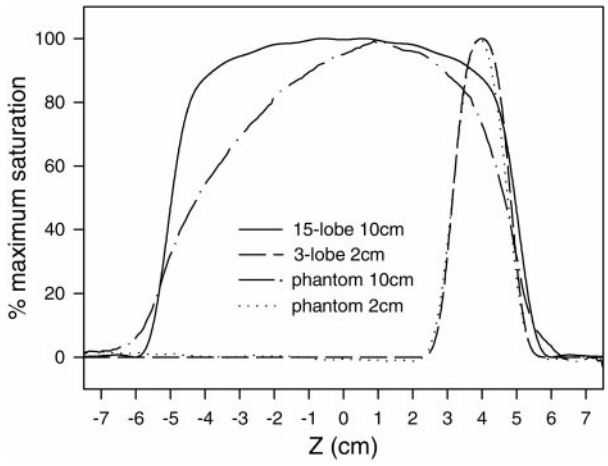

FIG. 3. Simulated and measured slice profiles of a 12.8-msec 15-lobe sinc pulse of 10-cm thickness as used in QUIPSS II and a 3.2-msec 3-lobe sinc pulse of 2-cm thickness as used in Q2TIPS, both with Hamming window weighting, scaled to maximum saturation. The imaging slices are located at the right side of the slice profiles with a 1-cm gap (not shown).

Perfusion maps averaged from raw difference images are shown in Fig. 4a for both QUIPSS II and Q2TIPS as a function of TI_1, together with the anatomical FLASH image and the IR-EPI image. GM pixels identified from the anatomical and IR-EPI images show high signal intensity in the perfusion maps. High-intensity pixels in the IR-EPI image, presumably cerebrospinal fluid (CSF), are dark in the perfusion maps. The averaged signals from the GM and WM ROIs at each value of TI_1 are shown in Fig. 4b. Q2TIPS signals in GM ROIs exhibit a linear dependence on TI_1, as described in Eq. [2], while QUIPSS II signals show higher intensity than Q2TIPS at all TI_1 values and have positive intercept at $TI_1 = 0$. This implies incomplete effectiveness of the QUIPSS II saturation pulse. The differences between QUIPSS II and Q2TIPS signals are greatest at short TI_1 and approach zero as TI_1 increases. For both pulse sequences, there is reduction of the amount of tagged blood that can be saturated as TI_1 increases because of outflow of blood from the tagged region. The differences between QUIPSS II and Q2TIPS signals are proportional to the amount of tagged blood that can be saturated. This suggests that most of the tag passes through the distal edge of the tagged region for TI_1 values greater than about 0.9 sec so that the saturation in this region, complete or not, does not change the perfusion signals significantly. WM signals are low and similar for both QUIPSS II and Q2TIPS at all TI_1 values. Figure 4c shows calculated CBF vs. TI_1 using Eq. [2] for all values of $TI_1 \leq 0.9$ sec and using Eq. [4] for $TI_1 = 1$ sec with an assumed τ of 0.9 sec. The standard deviation of the calculated GM CBF of all TI_1 values using Q2TIPS is 5.7% of the mean while it is 28% for QUIPSS II.

Multislice Q2TIPS

A set of perfusion maps for five contiguous slices with corresponding anatomical images is shown in Fig. 5 for $TI_1 = 0.7$ sec. All perfusion maps are on the same scale. Lower signal intensity in more distal slices is due to longer TI_2 since the images are sequentially acquired, proximal to distal. Q2TIPS signals of slices 1–5 from GM and WM ROIs are shown in Fig. 6a–e as a function of TI_1. GM Q2TIPS signals exhibit a linear dependence on TI_1 for $TI_1 < \tau$ for all five slices and level off for $TI_1 > \tau$ where τ is about 0.7 sec. The calculated CBF vs. TI_1 curves for all five slices are shown in Fig. 6f with an assumed τ of 0.7 sec for the last two TI_1 data points. The standard deviations of the calculated CBF of all TI_1 values for slices 1–5 are 4.3, 3.2, 5.8, 3.6, and 10.4% of the means.

Optimization of TI_{1S} and TR

Q2TIPS images at different TI_{1S} values with $TI_1 = 0.7$ sec are shown in Fig. 7a along with the anatomical FLASH image. Q2TIPS signals from GM and WM ROIs as a function of TI_{1S} are shown in Fig. 7b. For sufficiently long TI_{1S} values, Q2TIPS signals should be constant for fixed TI_1

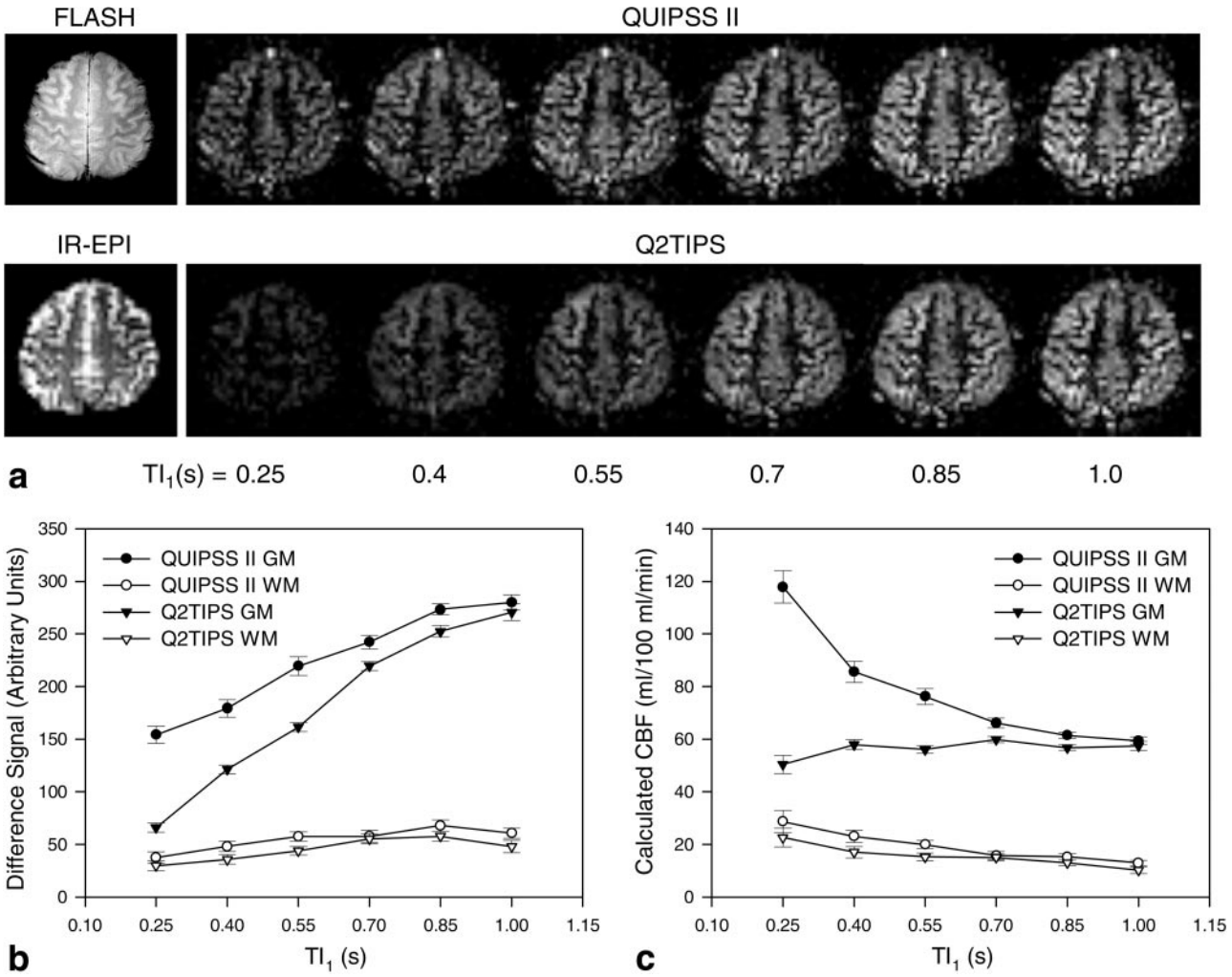

FIG. 4. Q2TIPS *vs.* QUIPSS II. **a:** Anatomical FLASH image, IR-EPI image, and QUIPSS II and Q2TIPS ΔM images with $TI_2 = 1.4$ sec while TI_1 is varied from 0.25 to 1 sec. **b:** QUIPSS II and Q2TIPS averaged ΔM *vs.* TI_1 from GM and WM ROIs. **c:** Calculated CBF from data in b using Eq. [1] for $TI_1 = 0.25$–0.85 sec and Eq. [3] for $TI_1 = 1$ sec with an assumed τ of 0.9 sec.

since the tail of the tag is completely saturated. If TI_{1S} is too short, tagged blood at the tail of the whole tag reaches the imaging slice. The inflection in this curve indicates the time at which the tail of the tag reaches the proximal end of the periodic saturation slice, which is between 0.825 and 0.925 sec in Fig. 7b. This is consistent with the inference from Fig. 4b that at about 0.9 sec most of the tagged blood passes through the tagged region since the location of the imaging slice relative to the RF coil is the same in both studies. WM Q2TIPS signals do not show significant dependence on TI_{1S}. Note the strong artifactual perfusion signal in the draining veins (arrows), which are dark in the anatomical image due to short T_2* at 3 T. Figure 7c shows the averaged signals vs. TI_{1S} from the pixels in these draining veins. These pixels were not included in the calculations for Fig. 7b. The artifactual perfusion signals in the draining veins are very high with short TI_{1S}, and decrease as TI_{1S} increases.

Figure 8 shows Q2TIPS signals vs. TR with $TI_1 = 0.7$ sec and $TI_{1S} = 1.05$ sec. The decrease in GM Q2TIPS signals at short TR values is because the tagged blood destined to perfuse the imaging slice is not completely replaced by the fully relaxed blood in the tagged region before the next inversion pulse.

DISCUSSION

Q2TIPS vs. QUIPSS II

QUIPSS II minimizes two systematic errors found in conventional pulsed ASL techniques—spatially varying transit delay and the flow-through effect—by introducing a saturation pulse between the inversion pulse and image acquisition. However, residual errors remain in the experimental data, as shown in Fig. 4.

Q2TIPS improves the accuracy of perfusion quantitation by replacement of the QUIPSS II saturation pulse with a train of thin-slice periodic saturation pulses applied at the distal end of the tagged region from TI_1 to TI_{1S}. Q2TIPS provides decreased B_1 sensitivity and an improved slice profile. With these improvements, the remaining error appears to be very small.

In Fig. 4b, the TI_1 time point where the QUIPSS II signal approaches the Q2TIPS signal depends on τ, which in turn

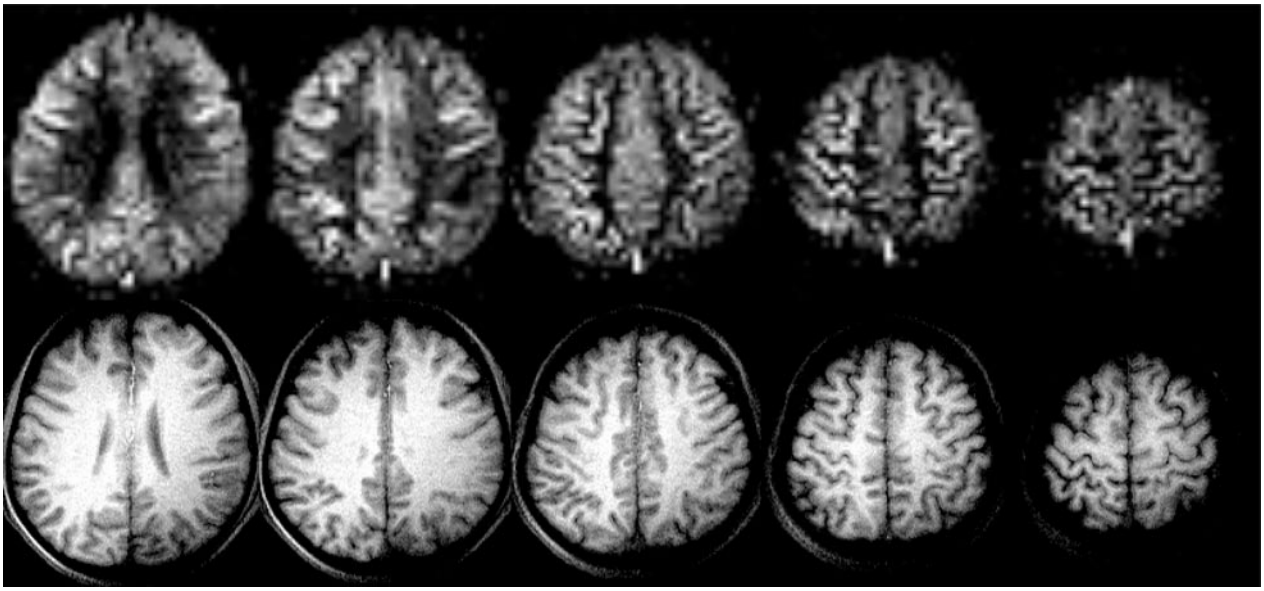

FIG. 5. Q2TIPS ΔM images of five contiguous slices with $TI_1 = 0.7$ sec, along with the corresponding anatomical reference images. The ΔM images are displayed on the same scale. Low signal intensity at more distal slices is due to longer image acquisition time (longer TI_2).

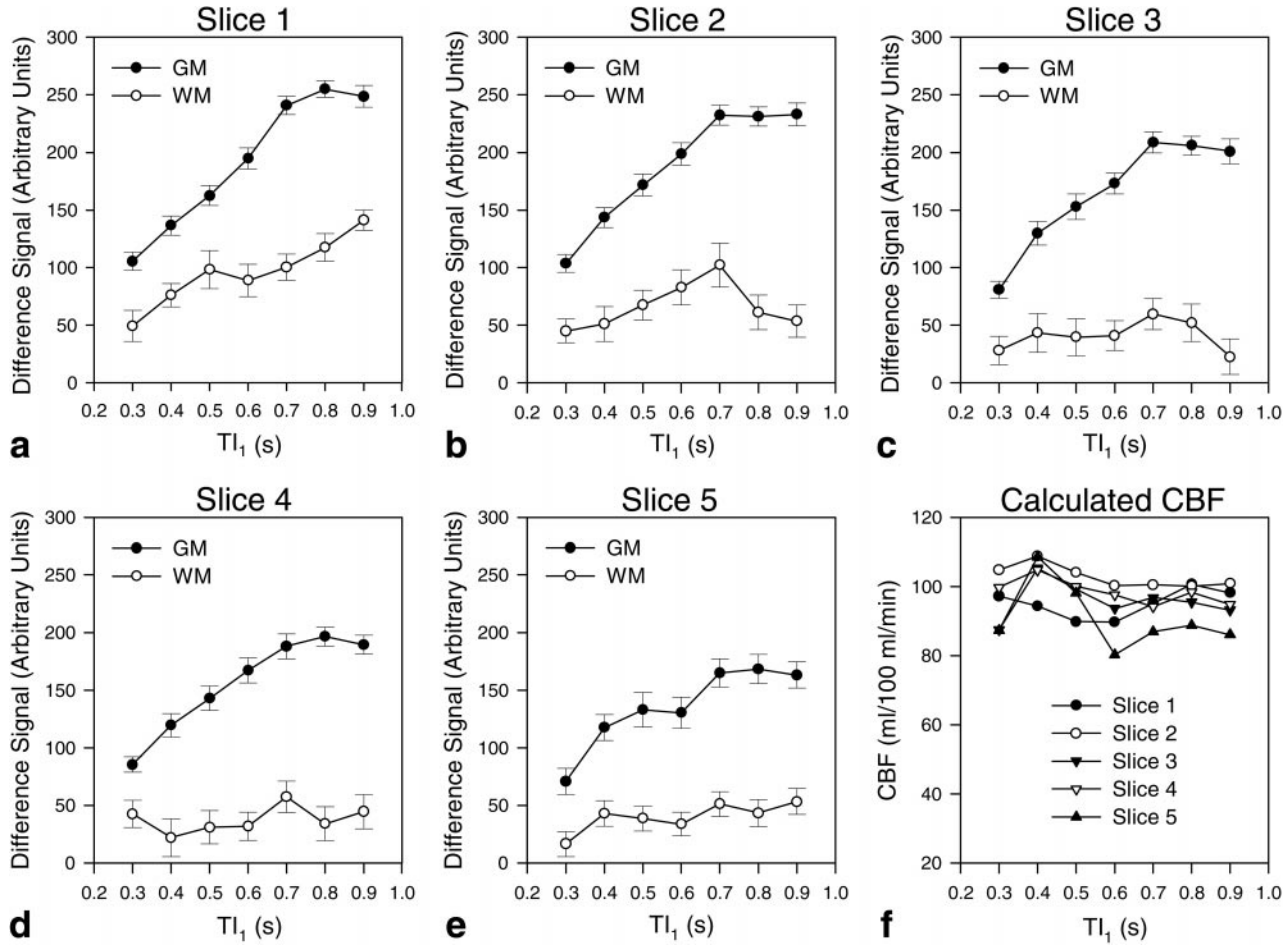

FIG. 6. **a**–**e:** Q2TIPS averaged ΔM from GM and WM ROIs for slices 1 to 5, respectively. **f:** Calculated CBF of GM ROIs using Eq. [1] for $TI_1 = 0.3$–0.7 sec and Eq. [3] for $TI_1 = 0.8$–0.9 sec with an assumed τ of 0.7 sec.

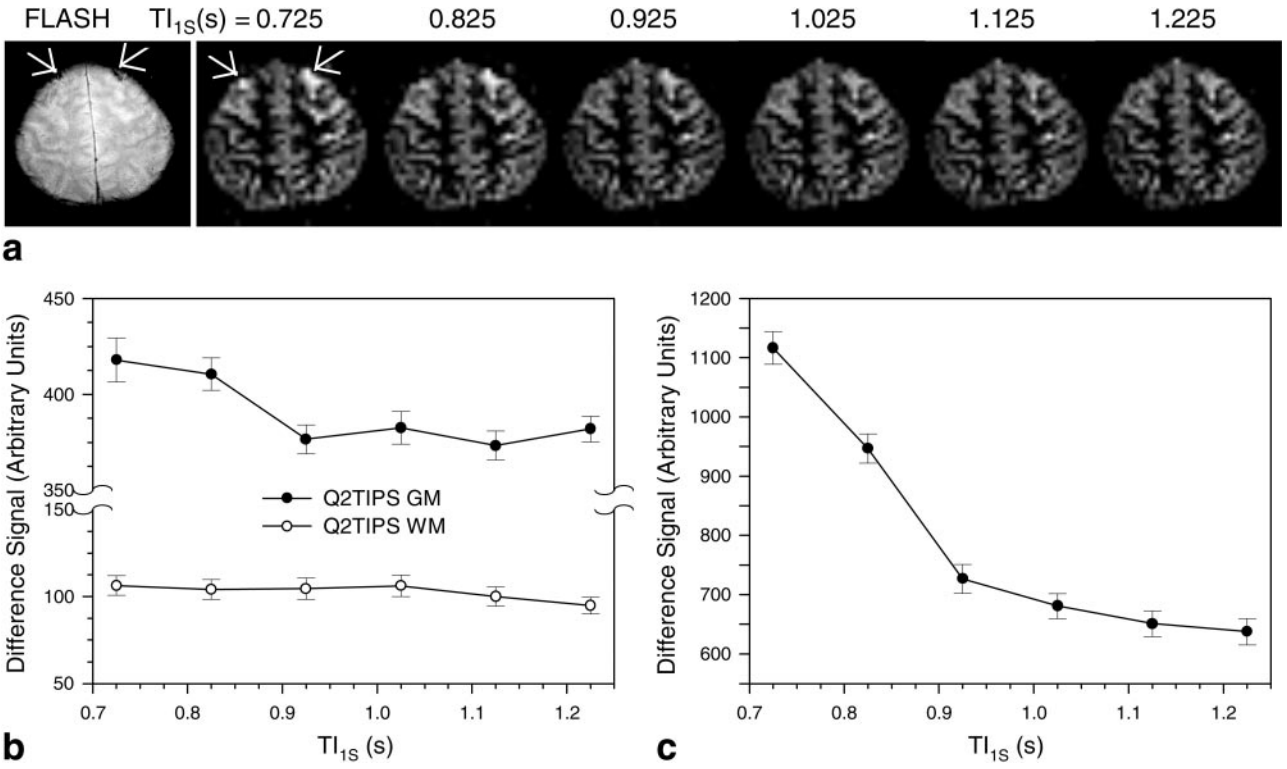

FIG. 7. **a:** Anatomical FLASH image and Q2TIPS ΔM images with $TI_1 = 0.7$ sec as a function of TI_{1S}. Pixels with draining veins (arrows) appear dark in the FLASH image and have high artifactual signals. **b:** Q2TIPS averaged ΔM vs. TI_{1S} from GM and WM ROIs. **c:** Q2TIPS averaged ΔM vs. TI_{1S} from pixels with high artifactual signals (arrows in a).

is related to the physical size of the tagged region. τ can also be estimated from the TI_1 time point in the GM Q2TIPS signal vs. TI_1 curves, as in Figs. 4b and 6a–e, where the linear dependence levels off as TI_1 increases. However, τ is not well defined within a voxel and has a wide distribution across pixels due to the dispersion of flow velocities. If shorter intervals between TI_1 data points were used, a smooth transition from linear dependence to linear independence should be observed in the Q2TIPS signal vs. TI_1 plot, providing that the SNR is sufficient.

Because the imaging slab is thicker in the multislice studies, the tagged region is more inferior than in the single-slice studies. The shorter τ in the multislice studies is due to the smaller tagged region since the proximal end of the tagged region is limited by the sensitive range of the RF coil used in the present studies. The calculated CBF when $TI_1 = 1$ sec in the single-slice studies and when $TI_1 = 0.8$ and 0.9 sec in the multislice studies depends on the estimates of τ. A TI_1 value that is shorter than τ should be used for the quantitation of perfusion in practice, and TI_2-TI_1 should be long enough to compensate for the variable transit delay as described in Eq. [3].

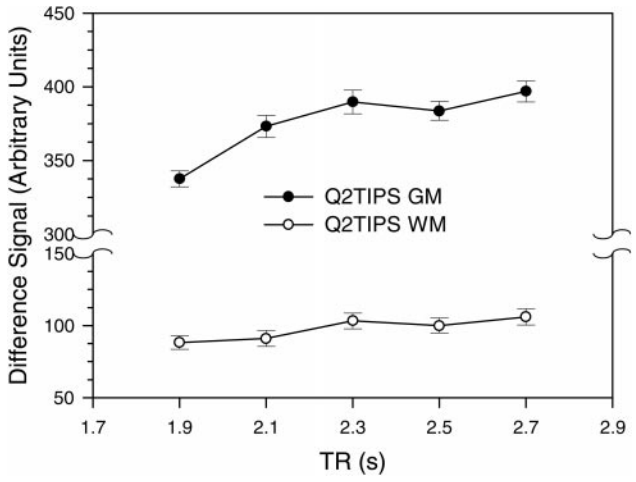

FIG. 8. Q2TIPS averaged ΔM vs. TR from GM and WM ROIs with $TI_1 = 0.7$ sec and $TI_{1S} = 1.05$ sec while TR is varied from 1.9 to 2.7 sec.

Multislice Q2TIPS

The calculated CBF values from five contiguous slices in Fig. 6f show good agreement at each TI_1 data point. This again demonstrates the improved accuracy using Q2TIPS for a 4-cm imaging slab with $TI_2 = 1.4$ sec. For a thicker imaging slab, a longer TI_2 value can be used to satisfy Eq. [3] at the expense of SNR. Although the correction using q, which is different for each slice, was not made and an assumed T_{1B} was used in the present calculations, these factors only cause the curves in Fig. 6f to shift with respect to the y-axis, and the relative relationships at each TI_1 data point do not change. The signals from more distal slices are noisier since fewer pixels are in the GM ROIs and the SNR is lower due to longer TI_2. In addition, Eq. [3] may not be fulfilled for slice 5 at long TI_1 values due to longer δt in more distal slices. WM perfusion signals are quite noisy in the multislice studies and may be affected by overlap of contiguous slices and partial voluming with GM.

Optimization of TI_{1S} and TR

The optimal TI_{1S} value is about 0.925 sec for the single-slice studies in Fig. 7b and should be even shorter for thinner tagged regions, as in the present multislice studies. TI_{1S} determines the minimum TR that can be applied since the arterial blood in the periodic saturation slice must be refreshed. Note that not all tagged blood perfuses the imaging slices. In the distal part of the tagged region, tagged blood in small arteries is likely to perfuse the imaging slices while blood in the large arteries is likely to pass through the imaging slices. Blood in small arteries in the proximal part of the tagged region is likely to perfuse local tissue while blood in the large arteries is likely to reach the imaging slices. It follows that only tagged blood destined for the imaging slices needs to be refreshed within a time TR.

There is a tradeoff between the size of the tagged region and TR. τ is proportional to the physical size of the tagged region. The minimum TR is TI_{1S} plus the time duration for the tagged blood to be refreshed in the periodic saturation slice, and this refreshing time duration is less than τ ($\text{minTR} < TI_{1S} + \tau$). The optimal TI_{1S} value is the time for the tail of the entire tag to reach the proximal end of the periodic saturation slice, and therefore is less than τ. It follows that the minimum TR is less than 2τ if the optimal TI_{1S} is used. If the optimal TI_1 is slightly shorter than τ, Eq. [3] becomes $TI_2 > \tau + \delta t$. This suggests a strategy for perfusion studies of more inferior imaging slices where the available size of the tagged region is small. Because τ is short in these studies, shorter TR and TI_2 values can be used for optimal SNR per unit time. An alternative strategy would be to use a longer RF coil.

A shorter TI_{1S} value can be employed for a thicker S_{nom} and therefore a shorter minimum TR, at the expense of a less sharp slice profile. For a given S_{nom}, the T_p value should be short enough to ensure complete saturation of the remaining tagged blood while keeping the RF power deposition below the FDA guideline. Although the tagged blood does not undergo simple plug flow and the blood vessels are generally curved, the tagged blood must pass through the periodic saturation slice to perfuse the imaging slices. The current implementation of a 2-cm periodic saturation slice applied every 25 msec allows saturation of tagged blood traveling perpendicularly across the periodic saturation slice with an average velocity less than 80 cm/sec, i.e., the cut-off velocity. For non-perpendicular pathways, tagged blood flowing at a higher velocity would be saturated. Moreover, faster flowing tagged blood that has a velocity higher than 80 cm/sec close to the imaging slices is likely to pass through the imaging slices by time TI_2 and be undetected since the periodic saturation slice is close to the imaging slices. Saturation with 2.5-cm five-lobe sinc saturation pulses was less complete than with the 2-cm three-lobe sinc pulses currently implemented (data not shown).

Possible Artifacts

The artifactual perfusion signals in draining veins as shown in Figs. 7a and c at short TI_{1S} are likely to come from the tagged venous blood in the tagged region rather than from tagged arterial blood (19). One advantage of Q2TIPS is the suppression of these artifactual signals. Tagged venous blood is likely to pass through the imaging slices at TI_2 since it accelerates through venous vessels. However, it would remain in the imaging slices longer if it were to run parallel within the imaging slices. In Q2TIPS, tagged venous blood is saturated if it arrives in the periodic saturation slice after TI_1 while tagged blood arriving before TI_1 is more likely to flow through the imaging slices. The example in Fig. 7c shows that the difference between the first and the last data points is from tagged venous blood that arrives at the periodic saturation slice between 0.725 and 1.225 sec. Note that two periodic saturation pulses were applied for the data point $TI_{1S} = 0.725$ sec in Fig. 7. Artifactual signals from venous tagged blood are more prominent when using EPISTAR, FAIR, and PICORE.

The PICORE tagging scheme used in the present studies provides control of the physical size of the tagged region if the proximal end of the specified tagged region is within the sensitive range of the RF coil. For the FAIR tagging scheme, the size of the tagged region depends on the location of the imaging slice relative to the proximal sensitive range of the RF coil and may be different among subjects. PICORE has the advantage of avoiding the complication of the signal contribution from the tagged spins coming from the distal side of the imaging slices. This signal is negative in EPISTAR, positive in FAIR, and zero in PICORE. In FAIR, the physical gap between the tagged region and the imaging slices can be thinner to realize a shorter δt and longer τ since the edge of the inversion slice profile is sharper for a thinner inversion slab. However, this may lead to increase of slow-flowing tagged venous blood in smaller veins entering the imaging slices and to increase of artifactual perfusion signals.

CONCLUSIONS

We have modified QUIPSS II to minimize the errors due to B_1 inhomogeneity and the mismatch of the slice profile of the saturation pulse to that of the inversion pulse. Q2TIPS improves the accuracy of perfusion quantitation as demonstrated in both single and multislice studies.

ACKNOWLEDGMENTS

This work was supported by grants MH51358 (to J.S.H.) and NS36211 (to E.C.W.) from the National Institutes of Health.

REFERENCES

1. Bandettini PA, Wong EC, Hinks RS, Tikofsky R, Hyde JS. Time course EPI of human brain function during task activation. Magn Reson Med 1992;25:390–397.
2. Kwong KK, Belliveau JW, Chesler DA, Goldberg IE, Weisskoff RM, Poncelet BP, Kennedy DN, Hoppel BE, Cohen MS, Turner R, Cheng HM, Brady TJ, Rosen BR. Dynamic magnetic resonance imaging of human brain activity during primary sensory stimulation. Proc Natl Acad Sci USA 1992;89:5675–5679.
3. Ogawa S, Tank DW, Menon R, Ellermann M, Kim S-G, Mekel H, Ugurbil K. Intrinsic signal changes accompanying sensory stimulation: functional brain mapping with magnetic resonance imaging. Proc Natl Acad Sci USA 1992;89:5951–5955.
4. Williams DS, Detre JA, Leigh JS, Koretsky AP. Magnetic resonance imaging of perfusion using spin inversion of arterial water. Proc Natl Acad Sci USA 1992;89:212–216.

5. Detre JA, Leigh JS, Williams DS, Koretsky AP. Perfusion imaging. Magn Reson Med 1992;23:37–45.
6. Alsop DC, Detre JA. Reduced transit-time sensitivity in noninvasive magnetic resonance imaging of human cerebral blood flow. J Cereb Blood Flow Metab 1996;16:1236–1249.
7. Ye FQ, Mattay VS, Jezzard P, Frank JA, Weinberger DR, McLaughlin AC. Correction for vascular artifacts in cerebral blood flow values measured by using arterial spin tagging techniques. Magn Reson Med 1997;37:226–235.
8. Alsop DC, Maccotta L, Detre JA. Multi-slice perfusion imaging using adiabatic arterial spin labeling and an amplitude modulated control. In: Proceedings of the ISMRM 5th Annual Meeting, Vancouver, 1997. p 81.
9. Ye FQ, Smith AM, Yang Y, Duyn J, Mattay VS, Ruttimann UE, Frank JA, Weinberger DR, McLaughlin AC. Quantification of regional cerebral blood flow increases during motor activation: a steady-state arterial spin tagging study. Neuroimage 1997;6:104–112.
10. Edelman RR, Siewert B, Darby DG, Thangaraj V, Nobre AC, Mesulam MM, Warach S. Qualitative mapping of cerebral blood flow and functional localization with echo-planar MR imaging and signal targeting with alternating radio frequency. Radiology 1994;192:513–520.
11. Edelman RR, Wielopolski P, Schmitt F. Echo-planar MR imaging. Radiology 1994;192:600–612.
12. Siewert B, Bly BM, Schlaug G, Darby DG, Thangaraj V, Warach S, Edelman RR. Comparison of the BOLD- and EPISTAR-technique for functional brain imaging by using signal detection theory. Magn Reson Med 1996;36:249–255.
13. Kwong KK, Chesler DA, Weisskoff RM, Rosen BR. Perfusion MR imaging. In: Proceedings of the SMR 2nd Annual Meeting, San Francisco, 1994. p 1005.
14. Kim S-G. Quantification of relative cerebral blood flow change by flow-sensitive alternating inversion recovery (FAIR) technique: application to functional mapping. Magn Reson Med 1995;34:293–301.
15. Kim S-G, Tsekos NV. Perfusion imaging by a flow-sensitive alternating inversion recovery (FAIR) technique: application to functional brain imaging. Magn Reson Med 1997;37:425–435.
16. Kim S-G, Ugurbil K. Comparison of blood oxygenation and cerebral blood flow effects in fMRI: estimation of relative oxygen consumption change. Magn Reson Med 1997;38:59–65.
17. Wong EC, Frank LR, Buxton RB. QUIPSS II: a method for improving quantitation of perfusion using pulsed arterial spin labelling. In: Proceedings of the ISMRM 5th Annual Meeting, Vancouver, 1997. p 1761.
18. Wong EC, Frank LR, Buxton RB. Quantitative multislice perfusion imaging using QUIPSS II, EPISTAR, FAIR, and PICORE. In: Proceedings of the ISMRM 5th Annual Meeting, Vancouver, 1997. p 85.
19. Wong EC, Buxton RB, Frank LR. Implementation of quantitative perfusion imaging techniques for functional brain mapping using pulsed arterial spin labeling. NMR Biomed 1997;10:237–249.
20. Wong EC, Buxton RB, Frank LR. Quantitative imaging of perfusion using a single subtraction (QUIPSS and QUIPSS II). Magn Reson Med 1998;39:702–708.
21. Dixon WT, Du LN, Faul DD, Gado M, Rossnick S. Projection angiograms of blood labeled by adiabatic fast passage. Magn Reson Med 1986;3:454–462.
22. Silver MS, Joseph RI, Hoult DI. Selective spin inversion in nuclear magnetic resonance and coherent optics through an exact solution of the Bloch-Riccati equation. Phys Rev A 1995;31:2753–2755.
23. Luh W-M, Wong EC, Bandettini PA, Hyde JS. QUIPSS II with thin-slice TI_1 periodic saturation (Q2TIPS): a method for improving accuracy of quantitative perfusion imaging. In: Proceedings of the ISMRM 6th Annual Meeting, Sydney, 1998. p 1191.
24. Frank LR, Wong EC, Buxton RB. Slice profile effects in adiabatic inversion: application to multislice perfusion imaging. Magn Reson Med 1997;38:558–564.
25. Buxton RB, Frank LR, Siewert B, Warach S, Edelman RR. A quantitative model for EPISTAR perfusion imaging. In: Proceedings of the SMR 3rd Annual Meeting, Nice, 1995. p 132.
26. Buxton RB, Wong EC, Frank LR. Quantitation issues in perfusion measurement with dynamic arterial spin labeling. In: Proceedings of the ISMRM 4th Annual Meeting, New York, 1996. p 10.
27. Cox RW. AFNI-software for analysis and visualization of functional magnetic resonance neuroimages. Comput Biomed Res 1996;29:162–173.